This article has been accepted for publication in a future issue of this journal, but has not been fully edited. Content may change prior to final publication. Citation information: DOI 10.1109/JIOT.2018.2828867, IEEE Internet of Things Journal

LoRaWAN: Evaluation of Link- and System-Level Performance

Luca Feltrin, Chiara Buratti, *Member, IEEE,* Enrico Vinciarelli,
Roberto De Bonis, *Member, IEEE* Roberto Verdone, *Member, IEEE,*

***Abstract*—The Internet of Things (IoT) addresses a huge set of possible application domains, requiring both short- and long-range communication technologies. When long distances are present, a number of proprietary and standard solutions for Low Power Wide Area Networks (LPWAN) are already available. Among them, LoRaWAN is a candidate technology supported by many network operators. This paper discusses the possible role of LoRaWAN for the IoT. First, the LoRaWAN technology is assessed experimentally through a set of laboratory and on-field tests, to characterize it from the link-level viewpoint; then, a system-level analysis is performed through simulation, to evaluate the capacity of a LoRaWAN gateway and a multi-gateway network to serve a large area. Finally, the results are discussed considering a broad set of use cases.**

***Index Terms*—Internet of Things (IoT), LoRa, LPWAN, Use Case, Protection Ratio, Capacity**

I. Introduction

THE Internet of Things (IoT) is emerging as a set of integrated technologies, new solutions and services, which are expected to change the way people live and produce (or benefit from) goods. The IoT paradigm, making all unmanned "things" (daily objects, industry machines, sensors, robots, animals, etc.) connected to the Internet, addresses a very large set of application domains. Some of them require short-range radio communication technologies (like Zigbee), being the network nodes confined in restricted areas; others, like precision agriculture, environmental monitoring, or animal tracking, may require communication solutions able to cover distances up to (or more than) 10 km in rural areas. Recently, the interest of industry towards the latter category, denoted as Low Power Wide Area Networks (LPWAN), grew significantly [1].

Some proprietary solutions, working on license-exempt spectrum bands, are already deployed in some regions: as an example, Sigfox[1] operates both as a technology and a service provider for LPWAN; another big player is the LoRa Alliance[2], which was officially established in Mobile World Congress 2015 and produced a proprietary solution known as LoRaWAN working in the license-exempt band, available in many countries, close to 900 MHz.

L. Feltrin, C. Buratti and R. Verdone are with DEI, University of Bologna, Italy, e-mails: {roberto.verdone, luca.feltrin, c.buratti}@unibo.it.

E. Vinciarelli and R. De Bonis are with TIM, Telecom Italia Mobile, Torino, Italy, emails: {enrico.vinciarelli, roberto.debonis}@telecomitalia.it.

[1]Sigfox, http://www.sigfox.com/en/

[2]LoRa alliance, https://www.lora-alliance.org/.

Meanwhile, the 3GPP is supporting three different LPWAN standards that will work on the licensed spectrum of mobile networks and will be commercially available by the end of 2017: Extended Coverage GSM (EC-GSM-IoT), LTE Machine Type Communications Category M1 (LTE-MTC Cat M1) and Narrowband IoT (NB-IoT). The latter technology has technical characteristics similar to LPWAN proprietary solutions, with the advantage of being a standard; many mobile network operators worldwide are supporting the development of NB-IoT, which might become a future reference IoT communication technology for several application domains. In the meanwhile, some network operators are pushing the LoRaWAN technology and supporting the developers' community [2].

In this context, made of many evolving technologies, it can be expected that a single one will not be capable of addressing efficiently all the different IoT use cases. It is in the interest of big players, to identify the range of applications that make a specific technology suitable. In particular, LoRaWAN is available since some time and industry is starting using it, but it is still not clear what are its true potentials. This paper shows results of an ongoing project developed at the University of Bologna supported by Telecom Italia Mobile, aimed at defining the technical limits of LoRaWAN and the opportunities it provides from both a link- and system-level points of view. As an outcome of this activity, LoRaWAN network capacity, defined in terms of maximum number of devices that can coexist in the same network, is assessed in single and multi-cell scenarios, under realistic traffic conditions.

Results show that only certain configurations are preferable to achieve high capacity, and the presence of multiple gateways improves considerably this performance indicator.

In Section II the main aspects of the LoRaWAN technology are presented. After a short overview of the most recent literature presented in Section III, section IV discusses how the results of few reference use cases can be extended to a broader set. In Section V the LoRa technology is assessed through a set of experimental laboratory and on-field tests, to characterize it from the link-level viewpoint. The information gathered during these experiments, in terms of ranging capabilities and interference resilience, is used in Section VI to discuss the design and performance of a network deployed, first, in a small area employing a single gateway, and then in a larger area. The paper draws final conclusions in Section VII.

This article has been accepted for publication in a future issue of this journal, but has not been fully edited. Content may change prior to final publication. Citation information: DOI 10.1109/JIOT.2018.2828867, IEEE Internet of Things Journal

TABLE I
DATARATE DEFINITION FOR EU863-870

Data Rate (DR)	Configuration	Indicative physical bit rate [bit/s]
DR0	SF12 / 125 kHz	250
DR1	SF11 / 125 kHz	440
DR2	SF10 / 125 kHz	980
DR3	SF9 / 125 kHz	1760
DR4	SF8 / 125 kHz	3125
DR5	SF7 / 125 kHz	5470
DR6	SF7 / 250 kHz	11000

II. LoRaWAN Technology

A. PHY Layer

LoRaWAN uses a proprietary modulation based on chirp spread spectrum, which exploits pulses whose frequency increases or decreases linearly over a certain amount of time; information is inserted in these pulses by introducing a discontinuity at different time offsets from the beginning of a symbol. These pulses occupy a bandwidth (BW) which can typically take values of 125, 250 or 500 kHz. Interference problems are mitigated by employing forward error correcting codes in combination with frequency hopping spread spectrum. For the simulations performed in this work, we considered a network using three 125 kHz bands, from 868 MHz to 868.6 MHz, corresponding to the EU868-870 sub-band G1.

One of the most important parameters affecting the performance at physical level is the Spreading Factor (SF), that is, the ratio between the signal bandwidth and the symbol rate. Keeping the bandwidth constant, it is possible to enhance the receiver sensitivity by increasing the time on air (duration of a packet transmission). More precisely, each increment of the SF by one unit, from the minimum value 6 to the maximum value 12, corresponds to a doubling of the time on air and a decrement of the receiver sensitivity of roughly three dB. As a reference case, with BW=125 kHz, the receiver sensitivity at the end device is -125 dBm and -137 dBm, for SF=7 and 12, respectively. Transmissions with different SFs are claimed to be orthogonal.

The documentation refers often to the Data Rate (DR) rather than the SF directly. In the LoRaWAN documentation framework, each DR value corresponds to a specific combination of SF and BW. This correspondence, defined in the LoRa Specifications [3], is reported in Table I. It is clear that, for most of the possible settings, an increment of the DR directly corresponds to a decrement of the SF [4], [5].

B. MAC Layer

The LoRaWAN MAC describes three Classes: i) Class A: end devices, after the transmission of a packet, open two receive windows to get an acknowledgement (ACK) or receive data from the gateway, then they stay in idle mode until the next transmission; ii) Class B: end devices have more receive windows synchronized with a beacon provided by the gateway; iii) Class C: end devices continuously stay in reception mode.

LoRaWAN networks form a star topology rooted at a LoRaWAN gateway, and any device has to be compliant with, at least, Class A (considered in this paper), where in uplink ALOHA protocol is used. There are two types of transmission mode: confirmed, using ACKs, and unconfirmed, when no ACKs are used. When an ACK is expected but not received by the transmitter, a recovery algorithm, which consists in multiple retransmissions, is initiated. The maximum number of retransmissions suggested in the specification is eight. Moreover, every two failed retransmissions DR is decremented; therefore, the SF increases and the time on air increases as well. This algorithm implicitly assumes that the transmission failed due to poor connectivity, therefore a lower DR should increment the success rate, as the receiver sensitivity will be better.

III. Literature

The scientific literature on LoRa, and LPWANs in general, is slowly expanding but most of the papers are still related to the link-level evaluation of the technology. Tests using Sigfox, LoRaWAN, and pre-standard NB-IoT solutions, have been made on the field by several network operators. Some field trials have been carried out, to determine LoRa ranging performance, in free space conditions [6] and in more complex scenarios [7].

Different studies have investigated the use of LoRa technology in specific fields of application, as for example, sailing monitoring systems [8], tactical troops tracking systems [9], smart cities [10], etc. In contrast with these works, we address a large set of applications, properly categorizing them.

Many details regarding the LoRa modulation and physical layer have been recently published in [11] and [12], where the Authors studied the output signal generated by commercial transceivers to understand how information is encoded and embedded in the chirp waveforms.

The interference problem has been addressed in [13], where the Authors study packet collisions applying a time offset between each other; in [14] and [1] the orthogonality of transmissions performed with different Spreading Factors, an important issue discussed in more detail in Section V, is studied mathematically. More precisely, in these articles the Authors analyze the architecture of the LoRa (de)modulator and determine the conditions for a capture to happen in the presence of two signals with different SF. We performed a similar analysis, but using an experimental approach.

The first papers about the system-level LoRa network capacity have been published very recently, most of them addressing the problem through simple mathematical approaches [15], [16]. In these works the limitations imposed by regulation on the utilization of the channel are taken into consideration as a major limit for the network capacity; although this is true when few continuously transmitting devices are considered, if the traffic generated is more sporadic and the number of devices is higher, this does not represent a problem. It is possible to show that among the use cases that we consider in this paper the channel utilization for a single device is always below 0.55%. Moreover, with respect to [15] and [16], we determine

This article has been accepted for publication in a future issue of this journal, but has not been fully edited. Content may change prior to final publication. Citation information: DOI 10.1109/JIOT.2018.2828867, IEEE Internet of Things Journal

the capacity of a network considering the full LoRa protocol stack, the presence of concurrent transmissions and consequent collisions or captures, and realistic information on the physical layer obtained through experiments.

In [17] the Authors estimated, through simulations, the capacity of a LoRa network assuming a simpler collision mechanism and protocol than what we used in this work; these assumptions lead to a lower capacity with respect to what we present in this paper.

In [18] the Authors studied experimentally the impact on the coverage of having multiple gateways deployed in a particular area of Glasgow. Our work, though, focuses more on capacity than on coverage: a fact of relevance for LoRa, whose receive sensitivity depends on transmission parameters (the Data Rate).

IV. LoRaWAN Key Vertical Markets

The space of potential LoRaWAN key vertical markets includes Smart Metering, Smart Grids, Smart Cities, Smart Homes, Agriculture, Tracking, Vehicle Telematics and Industrial applications [19]. However, while in some of these cases there are existing competing technologies, it is in the rural areas that the advantage of LoRaWAN, having a link budget tolerating power losses up to about 150 dB at 868 MHz, is the most valuable. In fact, the transmission range of a LoRaWAN gateway can be larger than 10 km; the same tolerance to power losses increases considerably the coverage capabilities in difficult areas, such as the basement of a building; this coverage condition is often referred to as "deep indoor". Therefore, for environmental monitoring, precision agriculture or animal tracking applications, LoRaWAN appears as a suitable candidate technology.

Moreover, the scarce spectral resources that LoRaWAN can use (in many countries, no more than 2 MHz of bandwidth), make it difficult to exploit it extensively in crowded environments, like cities where many private stakeholders might want to share the spectrum; in rural areas the opposite might be true, making the spectrum less crowded.

For these reasons, we focus our analysis on rural areas and related key applications. The set of applications for which LoRaWAN may be a well suited technology is still large, even when rural areas only are considered. In Table II we summarize these cases of interest, as they are defined in [20], indicating for each of them a target success rate, and we propose a grouping criterion in order to select few of them as representative for this work.

This criterion is based on traffic considerations, and in particular on the assumption that, given a payload size, and so a packet duration, a single gateway is able to process a certain number of packets per day approximately regardless to how many nodes are present in the network. This traffic, however, is the sum of the traffics generated by all devices in the network and the same amount of traffic can be generated by a high number of devices which rarely transmit a packet or few devices which transmit packets at a higher pace.

Based on this assumption, all the networks implementing use cases characterized by the same payload size will share the same ability to process their traffic. A common optimal amount of packets per day can be used to compute how many devices could be served individually, knowing how often they have a packet to transmit.

TABLE II
Application requirements for the use cases of interest.

Use Case	Packet rate (λ) [packet/day]	Minimum success rate ($P_{s,min}$)	Grouping
Wearables	10	90%	
Smoke Detectors	2	90%	
Smart Grid	10	90%	**Group A** $P_L = 10/20B$
White Goods	3	90%	
Waste Management	24	90%	
VIP/Pet Tracking	48	90%	
Smart Bicycle	192	90%	
Animal Tracking	100	90%	
Environmental Monitoring	5	90%	
Asset Tracking	100	90%	**Group B** $P_L = 50B$
Smart Parking	60	90%	
Alarms/Actuators	5	90%	
Home Automation	5	90%	
Machinery Control	100	90%	
Water/Gas Metering	8	90%	
Environmental Data Collection	24	90%	
Medical Assisted Living	8	99%	
Microgeneration	2	90%	
Safety Monitoring	2	99%	**Group C** $P_L = 100/200B$
Propane Tank Monitoring	2	90%	
Stationary Monitoring	4	90%	
Urban Lighting	5	90%	
Vending Machines Payment	100	90%	
Vending Machines General	1	90%	**Group D** $P_L = 1KB$

Therefore we can simulate only one case per group and use the results to compute the maximum number of devices that can be served for each individual use case, characterized by a different packet generation rate.

To prove the validity of this criterion, we assume a protection ratio[3] $\alpha = \infty$, N nodes in the network, each of them producing traffic at a given packet rate, denoted as λ [packet/day], with a constant delay between two consecutive transmissions. Each packet has a duration, or time on air (T_A), which is a function of the payload size denoted as P_L[4] [B].

Assuming that a device starts transmitting with a uniformly distributed time offset from $t = 0$, we can derive the following formula for the packet success rate, denoted as P_s, given by:

$$P_s = \left(1 - \frac{2T_A\lambda}{K_d}\right)^{N-1} \quad (1)$$

where K_d is a constant representing the number of seconds in a day and it is equal to 86400.

Figure 1 shows, as an example, P_s for six different use cases belonging to two different groups: Group B ($P_L = 50$ B) and Group C ($P_L = 100$ B), when the offered traffic $O = N\lambda$ [packet/day] is increasing, SF is set to 7. It is clear that use cases of the same group show a similar behavior in terms of success rate when the network traffic varies, which confirms the validity of our grouping criterion. When more complex protocols are employed by the devices, e.g. including retransmissions, the differences among the use cases of the same group tend to increase, but the above effect remains.

The representative use cases we selected for a deeper analysis are Waste Management in Smart cities for Group A, Animal Tracking for Precision Agriculture for Group B and Environmental Data Collection for Group C (see Table II).

[3]Properly defined later.

[4]The equation to calculate the packet time on air is described in [3].

This article has been accepted for publication in a future issue of this journal, but has not been fully edited. Content may change prior to final publication. Citation information: DOI 10.1109/JIOT.2018.2828867, IEEE Internet of Things Journal

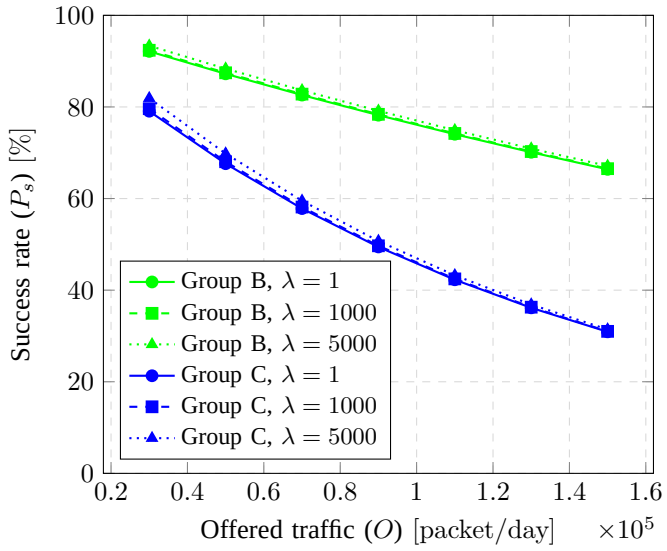

Fig. 1. Proof of concept for the grouping criterion

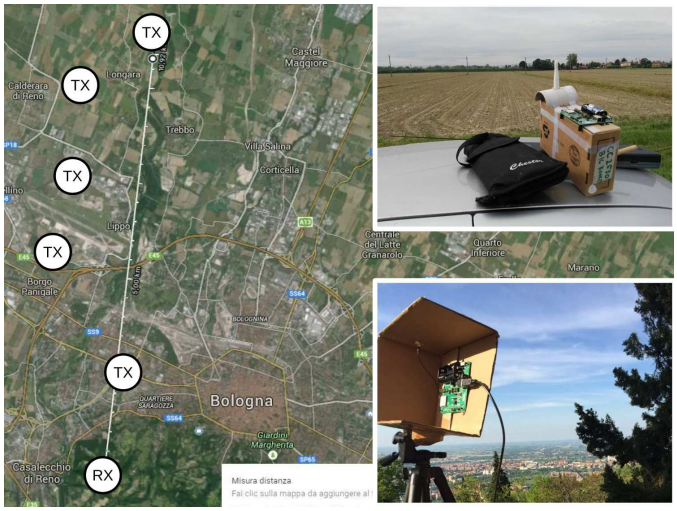

Fig. 2. Map of Bologna: setup for ranging experiments with fixed gateway.

V. Link Level Analysis

We performed two types of link-level assessment via experimentation, both needed to properly capture the link performance in system-level simulations. First, we measured the received power as a function of distance; then we assessed the claimed orthogonality of transmissions made with different SFs, and the protection ratio when the same SF is used by two simultaneously transmitting devices.

A. Experimental setup

In order to characterize the transmission range of a LoRa device we performed measurements of received power at increasing distances, with the aim to define a path loss model usable also in different conditions. Two Semtech SX1272 modules were used during this experiment, one deployed on a 240 m high hill and the other one, the transmitter, deployed in different locations at increasing distances in flat terrain (Figure 2). The maximum distance reached in this experiment was 10,8 km and for each location Line-Of-Sight (LOS) conditions[5] were met. The Received Signal Strength Indicator (RSSI) provided by the transceiver was used as a measurement of received power after being averaged over the transmission of 10,000 packets per location. The devices were configured to transmit using BW=250 kHz, coding rate 4/5, packets with a 18 byte payload and a transmit power $P_t = 14$ dBm. Measurements are discussed in sub-Section V-B.

In order to check the orthogonality among transmissions with different SFs, a wired test bed was setup using Semtech SX1272 as a receiver, and two Microchip RN2483 transceivers as transmitters. The experiments were conducted in a laboratory inspired to the methodology described in [21]. The two sources transmitted packets starting simultaneously, containing independent payload and using different SFs. The signal resulting from the mixing of the two transmitters outputs, is being duplicated, sent to the receiver and to a spectrum analyzer which is used to measure the Signal-to-Interference Ratio (SIR), defined as the ratio between the peak power of the intended received signal, and the peak power of the interfering signal. For each level of SIR, 10,000 packets were transmitted and the number of captured (i.e., correctly received) packets were counted, to assess the packet success rate. From the resulting curve, the protection ratio is derived as the value of SIR which implies a success rate of 50%.

The protection ratios found according to this methodology is representative only of a situation where no time offset is present between two colliding packets. Nevertheless it is expected that the presence of a time offset would reduce the overlap between the two packets and ultimately the amount of energy causing a collision. Therefore the results presented in this work can be considered as a worse case.

Measurement results are described in sub-Section V-C.

B. Transmission Range

Figure 3 presents the results of the measurements focused on the ranging capabilities of LoRa. Three dashed curves, one for each SF considered, show how the RSSI decreases as the distance increases; the SFs were chosen from the set $\{7, 9, 12\}$.

In the literature many channel models have been proposed to predict the path loss at 868 MHz, for example the Okumura-Hata model [22]. In Figure 3 we show also the expected received power according to the latter when the same scenario is considered, in ideal conditions.

We observed an almost constant difference between the ”Okumura-Hata” curve and our measurements: a gap of about 27 dB (Δ), which may be caused by antenna mismatches and other technological impairments. Assuming that this additional loss is present whenever the LoRa technology is involved, we consider from now on a path loss, L, given by the one predicted by the Okumura-Hata model (L_{OH}) increased by 27 dB; in other words $L = L_{OH} + \Delta$.

Overall, we estimated a path loss given by the following equation which corresponds to the curve ”Channel Model” in

[5]The first Fresnel ellipsoid was free from obstacles.

This article has been accepted for publication in a future issue of this journal, but has not been fully edited. Content may change prior to final publication. Citation information: DOI 10.1109/JIOT.2018.2828867, IEEE Internet of Things Journal

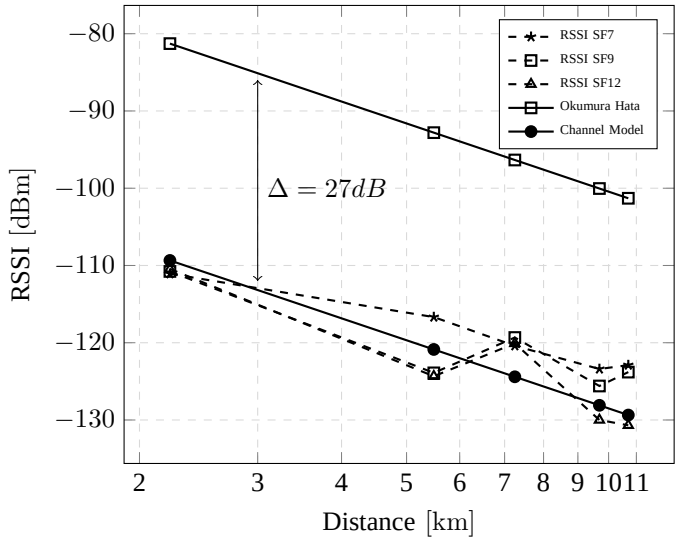

Fig. 3. Measured average RSSI [dBm] as a function of distance [km] and comparison with Okumura-Hata model.

TABLE III
LORA PROTECTION RATIOS IN dB.

		Useful Signal		
		SF7	SF9	SF12
Interfering Signal	SF7	0.3	-10.3	-11
	SF9	-13.8	0.3	-14.6
	SF12	< -30	-21.6	1.7

Figure 3: $L = 113.2 + 29.3\log_{10}(d_{km})$. Being the Okumura-Hata formula dependent on the device height and the type of scenario, also our model is inheriting the same dependencies [22].

C. Orthogonality of Spreading Factors

The SFs used by the devices were chosen in the set $(7, 9, 12)$. A first measurement campaign was conducted, letting the two transmitters use the same SF. In this case the lack of orthogonality brings to packet losses, as long as the SIR is not sufficiently large. Only minor differences were found when varying the SF. Defining conventionally the protection ratio, α, as the value of SIR that ensures a success rate equal to 50%, we then found it varies from 0.3 dB to 1.7 dB (see Table III).

A second campaign was conducted to study the assumption of orthogonality among transmissions performed using different SF. In Table III we report the estimated protection ratios in dB for all the cases already mentioned. As expected, the impact of the interferer on the useful transmissions is much smaller, but in any case different SFs are not perfectly orthogonal.

The effect of this lack of orthogonality may have an impact when a large network is considered; for example, in a network where all devices use the same transmit power, an interferer which is from 2 to 5 times closer to the gateway than another device, may cause a collision even when a different SF is used.

In the literature the possibility to have virtual orthogonal sub-channels is often mentioned, but some of the devices working in a given sub-channel will always be potential interferers for another set of devices working in a different sub-channel, depending on their relative positions. However, this phenomena can be considered as a second order effect since collisions due to the random access within the same sub-channel have a much stronger impact.

VI. SYSTEM LEVEL ANALYSIS

A. Simulator

We built a system-level simulator accounting for the main features of LoRaWAN MAC and the link-level aspects discussed above. We assume the area to cover is a square of side S, where N sensors are deployed randomly and uniformly. We also account for log-normal shadowing with standard deviation $\sigma = 2$, a coherence time $T_C = 200\ s$, and a negative exponential autocorrelation function [23], while the path loss is calculated according to Section V and considering the gateway(s) to be placed at a height of $30\ m$ from the ground. As already mentioned in Section V-B the different height has an impact on the path loss formula which can be reformulated in our case as $L = 127.6 + 35.22\log_{10}(d_{km})$.

Different scenarios characterized by a different number of gateways is considered. When multiple gateways are deployed they may receive multiple replicas of the same packet; in that case only one reception is considered in the final statistics.

The nodes wake-up, sample and transmit their data through the LoRaWAN access mechanism at regular time intervals which depend on λ as described in Section IV.

The simulator is event-based, therefore the packets are transmitted without any time quantization. A packet is detected by a device if the received power is greater than the sensitivity, if this happens the device will lock to the preamble and will try to decode the payload. When a collision between more packets happens, with any time offset, their SIR is calculated and the payload is passed to the upper layers if the device is locked to that particular packet and if the SIR is greater than the protection ratio estimated in Section V-C. In each device the main layers of the LoRaWAN standard are implemented as state machines. Each Gateway is equipped with parallel receivers, one for each channel and SF available; in this way it is able to process concurrent transmissions provided that a receiver is not busy handling another link.

To emphasize the role of proper link-level considerations, we used the simulator to compute the curves previously shown in Figure 1. The resulting curves are closer to a more realistic value with an absolute difference from the theoretical ones between 20% and 40%.

The most important simulation outputs consist in the success rate P_s, calculated as the ratio between the number of packets correctly received by the network and those transmitted by the devices, and the network throughput, T, calculated as the quantity of information correctly received by the network per unit of time: $T = \frac{P_L \lambda P_s}{K_d}$ [B/s].

Network capacity will be defined later based on discussions about the relationship between P_s, T and the offered traffic O. This will also require the identification of the best transmission mode (initial SF, confirmed or unconfirmed) for each use case/scenario considered.

This article has been accepted for publication in a future issue of this journal, but has not been fully edited. Content may change prior to final publication. Citation information: DOI 10.1109/JIOT.2018.2828867, IEEE Internet of Things Journal

B. Capacity of a small area

We considered a scenario consisting in a square area of 1 km^2 where a variable number of nodes is deployed and a LoRa gateway, placed in the center, is sufficient to cover all of them using any SF. For each group of use cases we vary the number of nodes to simulate different amounts of offered traffic. Let us define the network capacity as the amount of offered traffic which allows to maximize the network throughput. In Figure 4 we report four curves representing how the network throughput varies as the number of devices, and therefore the offered traffic, increases. Each curve represents a different configuration of the PHY and MAC parameters: confirmed or unconfirmed mode and initial SF equal to 7 or 12. In case of retransmissions, the SF increases as mentioned in Section II. For the sake of simplicity we only show the results for the use cases of Group B.

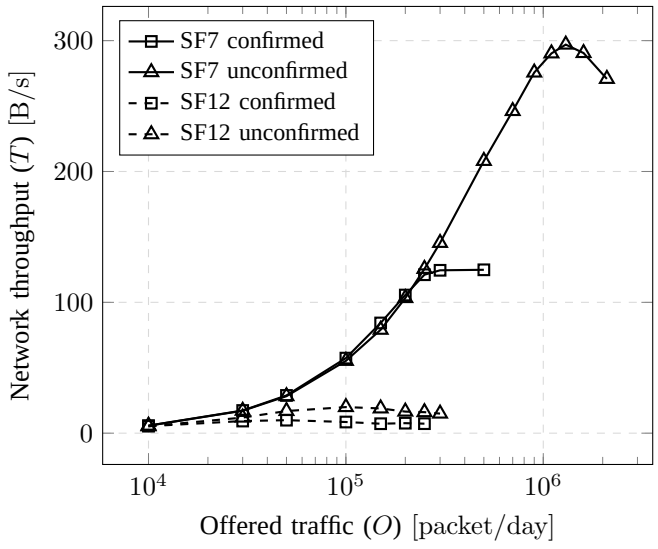

Fig. 4. Simulations: network throughput for Group B ($P_L = 50B$, $\lambda = 100$ packet/day).

It is evident that initial SF equal to 7 and unconfirmed mode is the configuration that allows the highest throughput which, for Group B, is around 300 B/s when the offered traffic is 1.3×10^6 packet/day. This is because of the small area size.

The problem with this definition of capacity, though, is that it leads to an operating point where the packet success rate is around 39% for the case of Group B, which is too low for many applications. The same happens also for the other groups. For this reason we redefine the network capacity, O_{max}, as the maximum amount of offered traffic O which guarantees a given level of packet success rate $P_{s,min}$.

Figures 5, 6 and 7 show how the packet success rate changes when the offered traffic increases for the three groups and for each different configuration used.

Generally speaking, in case of a small area to cover, the best solution is to set the SF to 7 in order to avoid collisions by keeping the packet time on air, and so the SF, as small as possible. Moreover, when there is not much traffic in the network, the confirmed mode is the best choice to guarantee a high success rate.

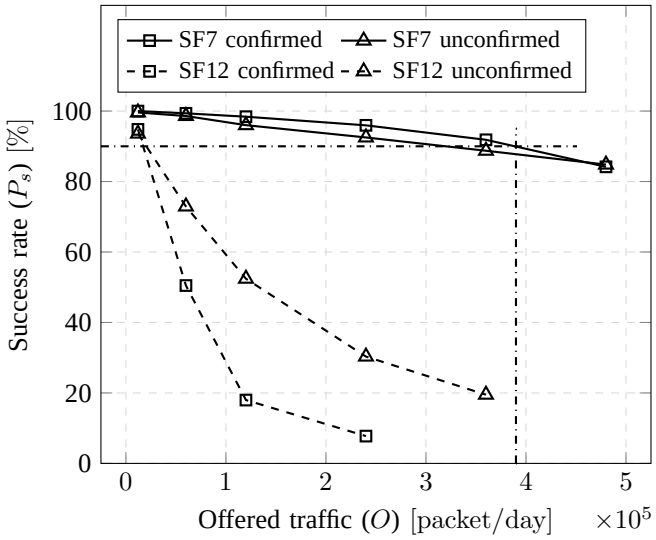

Fig. 5. Simulations: success rate for Group A ($P_L = 10B$, $\lambda = 24$ packet/day).

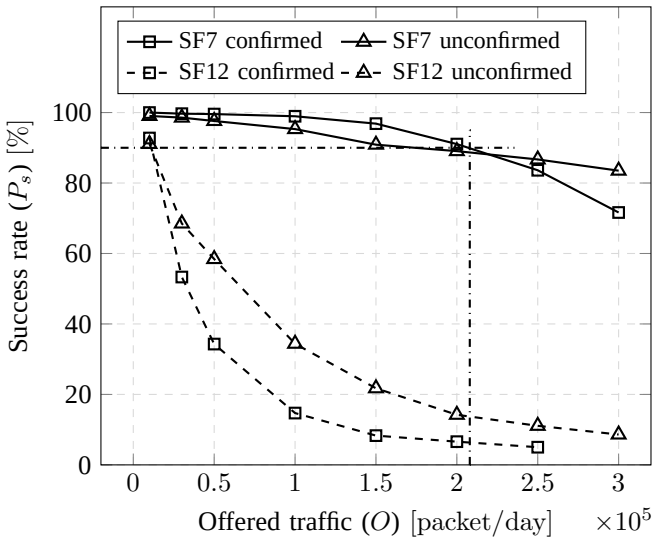

Fig. 6. Simulations: success rate for Group B ($P_L = 50B$, $\lambda = 100$ packet/day).

When the network is more congested, the retransmission mechanism increases the collision probability which leads to a lower success rate and throughput; for this reason the curves for SF7 and confirmed mode become lower than the curves for SF7 and unconfirmed mode when the offered traffic becomes higher than a certain value. This can be observed easily in Figures 5 and 6, while in Figure 7 this phenomena happens at higher amounts of offered traffic.

From these curves, considering the desired minimum success rates reported in Table II, we derived the network capacity for the different use case groups; this capacity is always reached when confirmed mode and SF7 are used. All the resulting capacities are reported in Table IV. For each use case the maximum number of devices that guarantees the required success rate can be calculated as $N_{max} = O_{max}/\lambda$. Moreover,

This article has been accepted for publication in a future issue of this journal, but has not been fully edited. Content may change prior to final publication. Citation information: DOI 10.1109/JIOT.2018.2828867, IEEE Internet of Things Journal

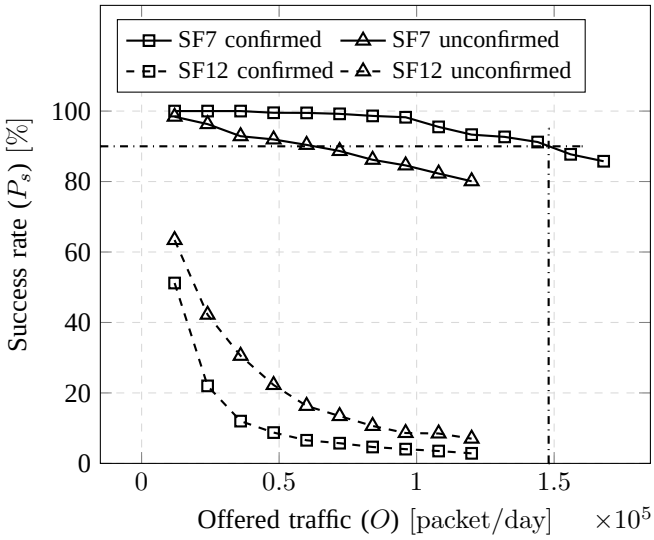

Fig. 7. Simulations: success rate for Group C ($P_L = 200B$, $\lambda = 24$ packet/day).

TABLE IV
NETWORK CAPACITY FOR THE USE CASES OF INTEREST IN A SMALL AREA.

Use Case	Network capacity (O_{max}) $\times 10^3$ [packet/day]	Network size (N_{max}) $\times 10^3$ [devices]	Node Density (ρ_{max}) [devices/hectare]
Wearables	390	39	390
Smoke Detectors	390	195	1950
Smart Grid	390	39	390
White Goods	390	130	1300
Waste Management	390	16.3	163
VIP/Pet Tracking	208	4.33	43.3
Smart Bicycle	208	1.08	10.8
Animal Tracking	208	2.08	20.8
Environmental Monitoring	208	41.6	416
Asset Tracking	208	2.08	20.8
Smart Parking	208	3.47	34.7
Alarms/Actuators	208	41.6	416
Home Automation	208	41.6	416
Machinery Control	208	2.08	20.8
Water/Gas Metering	148	18.5	185
Environmental Data Collection	148	6.17	61.7
Medical Assisted Living	75[6]	9.38	93.8
Microgeneration	148	74	740
Safety Monitoring	75[6]	37.5	375
Propane Tank Monitoring	148	74	740
Stationary Monitoring	148	37	370
Urban Lighting	148	29.6	296
Vending Machines Payment	148	1.48	14.8
Vending Machines General	-	-	-

the maximum node density compatible with the requirement is given by $\rho_{max} = N_{max}/S^2$. These results are shown in Table IV as well.

The average latency, defined as the average delay between the request of transmission at device side and the notification to the application layer of correct reception at gateway side, is 4.1, 6.9 and 7.8 seconds for Groups A, B and C, respectively. This high latency is due to the retransmission mechanism employed to achieve the higher capacity, but it can be easily reduced below one second by using unconfirmed mode which cause a drop in the success rate of less than 10%.

[6]Note that these two use cases have a more strict requirement in terms of success rate.

C. Coverage of a large area

Let us assume to have a scenario where the area to cover is larger. As we already discussed, a solution to the problem may be to increase the SF used by the devices; in this way the transmission range of the devices is larger but the radio channel is utilized more intensively due to longer packet durations, a behavior that can lead quickly to the saturation of the network. Another solution is to deploy more gateways in the territory; this allows us both, to cover a larger area without the need for the devices to use a high SF, and also to help the network process the traffic when the channel is congested.

According to the LoRaWAN specification, when a device sends a packet, potentially all gateways in the network could receive it. It is sufficient that only one is received to succeed. This implies that the higher is the amount of gateways in the networks, the higher is the success rate.

Before analyzing the network capacity, a set of simulations has been performed to study the benefits of having multiple gateways; the scenario considered is a square area of side $S = 6.82\ km$, which is represented in Figure 8; the gateways are disposed in a hexagonal grid and every cell has a radius $R_{cell} = 1.97\ km$ which corresponds to the average transmission range of a LoRa device considering the downlink, SF7 and the channel path loss formula already used in the previous section. Simulations are performed by varying the number of sinks deployed, in particular a scenario with only gateway A is considered first, then a network with only four gateways (A, B, C and D), and finally one with all seven gateways deployed. Notice that when all gateways are considered the area is fully covered with SF7, while when only gateway A is present a SF higher than 10 is needed to cover the area. The devices in the network generate an offered traffic (O) of approximatively 112 thousands packet/day.

Figure 9 shows how the success rate increases as the number of gateways employed rises. All the curves shown represent the performance of the network when unconfirmed mode is selected. The dashed curves are made considering initial $SF = 7$ while the solid ones considering initial $SF = 12$.

When the initial SF is 7 the network is not congested, therefore every packet is received by a gateway that is simply within the transmission range of the sender; in this case the improvement in terms of success rate, represented by the dashed lines, is given by a better geometrical coverage provided by the additional gateways. This can be seen also by comparing the three curves with the "Geometrical Coverage" curve, which represents the fraction of the area defined by the union of all the circles centered in the gateway locations and with radius equal to the transmission range with SF7, with respect to the total area. This curve is very close to those mentioned above, proving that all the effects related to the MAC protocol are negligible.

When the initial SF is 12, the geometrical coverage is always 100%, so the improvement represented with the solid lines is only due to the higher probability of having at least one packet received with a signal to interference ratio higher than the protection ratio. This improvement is similar among the three groups; their success rates differ only in the absolute

This article has been accepted for publication in a future issue of this journal, but has not been fully edited. Content may change prior to final publication. Citation information: DOI 10.1109/JIOT.2018.2828867, IEEE Internet of Things Journal

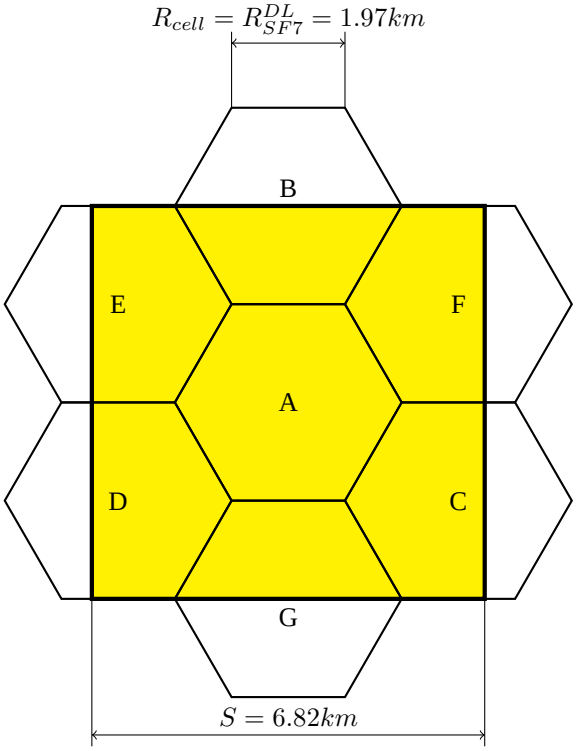

Fig. 8. Scenario with multiple gateways.

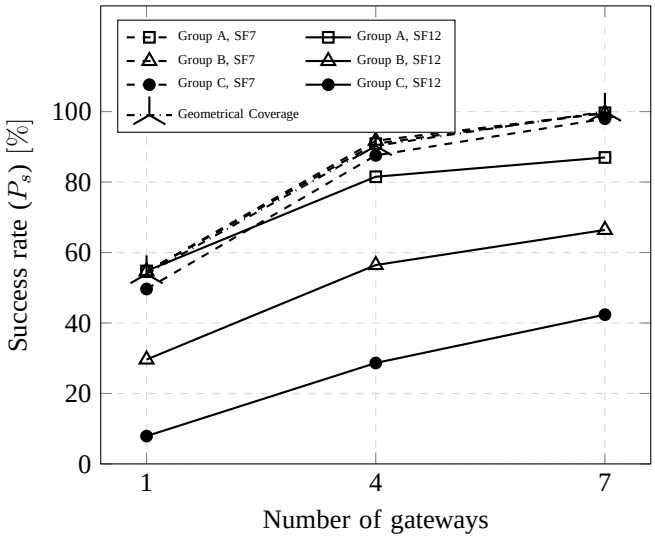

Fig. 9. Success rate for the three groups as a function of the number of gateways.

value due to the different payload sizes which cause different levels of congestion when the offered traffic (O) is fixed, as in this case.

The previous statement can be confirmed also by observing the set of points representing the case with only one gateway deployed; this case differs from the one discussed in the previous section only in the size of the area. The success rates when the initial $SF = 12$ are identical in both scenarios, being the transmission range enough to cover all the devices in both cases, while with initial $SF = 7$ the success rate values are close to the amount of area in range, 100% when the area is small, 55% when it is large.

It is evident that, for the scenario proposed, the option that guarantees the highest success rate, therefore network capacity, is to use seven gateways and SF7.

D. Capacity of a large area

We now move to the characterization of P_s versus O as done in Section VI-B, this time varying the number of gateways in order to estimate how the network capacity improves when a more complex network is considered. For the sake of simplicity we consider only Group C and SF7. The four curves in Figure 10 represent the behavior of the network when confirmed or unconfirmed mode is used and when the number of gateways varies from one to four.

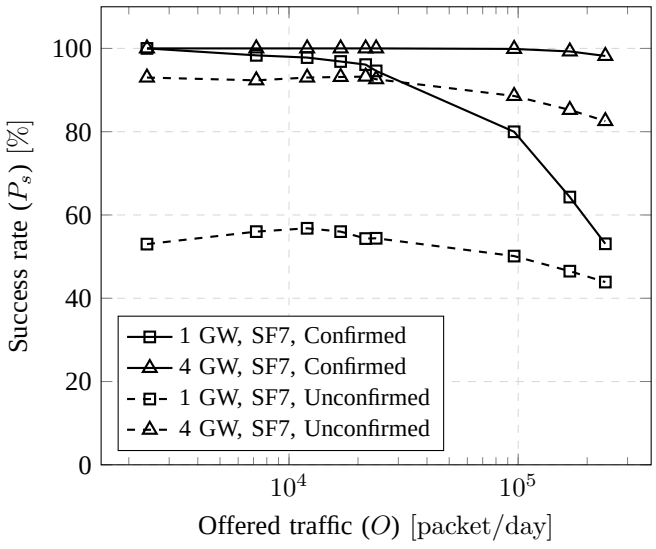

Fig. 10. Simulations: success rate for Group C with different number of Gateways ($P_L = 200B$, $\lambda = 24$ packet/day).

When unconfirmed mode is used the amount of traffic has a minor impact on the success rate as the geometrical coverage plays the main role, resulting in a success rate of 55% or 93% depending on the number of gateways.

When confirmed mode is used the coverage problem is overcome, therefore the success rate is limited only by capacity issues. When only one gateway is present, the success rate requirement ($P_{s,min} = 90\%$) is satisfied with an offered traffic smaller than $O_{max} = 40$ thousands packet/day, a significantly smaller value with respect to the scenario described in Section

This article has been accepted for publication in a future issue of this journal, but has not been fully edited. Content may change prior to final publication. Citation information: DOI 10.1109/JIOT.2018.2828867, IEEE Internet of Things Journal

TABLE V
NETWORK CAPACITY FOR THE USE CASES IN GROUP C IN A LARGE AREA.

Use Case	Network capacity (O_{max}) $\times 10^3$ [packet/day]	Network size (N_{max}) $\times 10^3$ [devices]	Node Density (ρ_{max}) [devices/hectare]
1 Gateway			
Water/Gas Metering	40	5	1.07
Environmental Data Collection	40	1.67	0.358
Medical Assisted Living	4.8	0.6	0.129
Microgeneration	40	20	4.3
Safety Monitoring	4.8	2.4	0.516
Propane Tank Monitoring	40	20	4.3
Stationary Monitoring	40	10	2.15
Urban Lighting	40	8	1.72
Vending Machines Payment	40	0.4	0.086
4 Gateways			
Water/Gas Metering	1500	188	40.3
Environmental Data Collection	1500	62.5	13.4
Medical Assisted Living	190	23.8	5.11
Microgeneration	1500	750	161
Safety Monitoring	190	95	20.4
Propane Tank Monitoring	1500	750	161
Stationary Monitoring	1500	375	80.6
Urban Lighting	1500	300	64.5
Vending Machines Payment	1500	15	3.22

VI-B because more devices tend to use a higher SF in order to reach the gateway. When four gateways are present, the minimum success rate is reached with an offered traffic $O_{max} = 1.5$ million packet/day, much higher than the case with only one gateway.

In Table V we report the capacity (O_{max}), the size (N_{max}) and the maximum node density (ρ_{max}) of a network implementing the use cases of Group C.

VII. CONCLUSIONS

We have assessed the capacity of a LoRaWAN network for a broad range of use cases of interest, specifically focusing on rural environments. This has been achieved through an experimental assessment of the link-level characteristics of the system, followed by a system-level simulation implementing all LoRaWAN specifications.

With reference to each use case, network capacity has been defined based on requirements on the success probability and the transmission rates of nodes.

Two separate scenarios have been analyzed, of very different size. In the smaller case, where one single gateway is used, as might be expected we found that optimal configuration of the network is achieved by setting lower values of SF, using confirmed mode. In the case of a larger scenario, we analyzed the network capacity obtained with one or more gateways. In the former case, as expected, network capacity is severely degraded, due to the need to use larger (and less efficient) values of SF; in the latter, a significant improvement is found.

More precisely, let us make reference to a specific use case, as an example: water/gas monitoring. When one gateway covers an area of one square km, the maximum density of nodes compatible with the application requirements is 185 nodes/hectare. If the same gateway is used in a much larger area (of size equal to about 46.5 square km) the maximum node density is significantly decreased: it is close to 1 node/hectare, a value reduced by a factor much larger than the area size. The reason stands in the need to use larger values of SF to cover far nodes, bringing to a much smaller efficiency in the use of the spectral resource. On the other hand, using in the same large area four gateways instead of one, introduces a notable improvement in network capacity: the maximum node density is about 40 nodes/hectare, that is, greater by a factor much higher than the number of additional gateways.

The analysis performed provides useful insights for the development of LoRaWAN networks.

VIII. ACKNOWLEDGMENT

The Authors wish to thanks Stefan Mijovic and Andrea Skajkic for the helpful discussions.

REFERENCES

[1] C. Goursaud and J.-M. Gorce, "Dedicated networks for IoT : PHY / MAC state of the art and challenges," *EAI endorsed transactions on Internet of Things*, Oct. 2015. [Online]. Available: https://hal.archives-ouvertes.fr/hal-01231221
[2] Orange, "LoRa Device Developer Guide," Tech. Rep., April 2016.
[3] LoRa Alliance, "LoRaWAN specification," January 2015.
[4] Semtech, "AN1200.22 LoRa Modulation Basics," May 2015.
[5] Semtech, "Datasheet SX1272/73 - 860 MHz to 1020 MHz Low Power Long Range Transceiver," March 2015.
[6] M. Aref and A. Sikora, "Free space range measurements with semtech LoRa^{TM}technology," in *Wireless Systems within the Conferences on Intelligent Data Acquisition and Advanced Computing Systems: Technology and Applications (IDAACS-SWS), 2014 2nd International Symposium on*, Sept 2014, pp. 19–23.
[7] J. Petajajarvi, K. Mikhaylov, A. Roivainen, T. Hanninen, and M. Pettissalo, "On the coverage of LPWANs: range evaluation and channel attenuation model for lora technology," in *ITS Telecommunications (ITST), 2015 14th International Conference on*, Dec 2015, pp. 55–59.
[8] L. Li, J. Ren, and Q. Zhu, "On the application of LoRa LPWAN technology in sailing monitoring system," in *2017 13th Annual Conference on Wireless On-demand Network Systems and Services (WONS)*, Feb 2017, pp. 77–80.
[9] W. San-Um, P. Lekbunyasin, M. Kodyoo, W. Wongsuwan, J. Makfak, and J. Kerdsri, "A long-range low-power wireless sensor network based on U-LoRa technology for tactical troops tracking systems," in *2017 Third Asian Conference on Defence Technology (ACDT)*, Jan 2017, pp. 32–35.
[10] V. A. Stan, R. S. Timnea, and R. A. Gheorghiu, "Overview of high reliable radio data infrastructures for public automation applications: LoRa networks," in *2016 8th International Conference on Electronics, Computers and Artificial Intelligence (ECAI)*, June 2016, pp. 1–4.
[11] B. Sikken. (2016) Decoding LoRa. [Online]. Available: https://revspace.nl/DecodingLora
[12] M. Knight and B. Seeber, "Decoding LoRa: Realizing a modern LPWAN with SDR," 2016.
[13] M. Bor, J. Vidler, and U. Roedig, "LoRa for the Internet of Things," in *Proceedings of the 2016 International Conference on Embedded Wireless Systems and Networks*, ser. EWSN '16, 2016, pp. 361–366.
[14] O. Georgiou and U. Raza, "Low power wide area network analysis: Can LoRa scale?" *IEEE Wireless Communications Letters*, vol. PP, no. 99, pp. 1–1, 2017.
[15] K. Mikhaylov, J. Petaejaejaervi, and T. Haenninen, "Analysis of capacity and scalability of the lora low power wide area network technology," in *European Wireless 2016; 22th European Wireless Conference*, May 2016, pp. 1–6.
[16] F. Adelantado, X. Vilajosana, P. Tuset-Peiró, B. Martínez, and J. Melià, "Understanding the limits of lorawan," *CoRR*, vol. abs/1607.08011, 2016. [Online]. Available: http://arxiv.org/abs/1607.08011
[17] M. C. Bor, U. Roedig, T. Voigt, and J. M. Alonso, "Do LoRa low-power wide-area networks scale?" in *Proceedings of the 19th ACM International Conference on Modeling, Analysis and Simulation of Wireless and Mobile Systems*, ser. MSWiM '16. New York, NY, USA: ACM, 2016, pp. 59–67. [Online]. Available: http://doi.acm.org/10.1145/2988287.2989163
[18] A. J. Wixted, P. Kinnaird, H. Larijani, A. Tait, A. Ahmadinia, and N. Strachan, "Evaluation of LoRa and LoRaWAN for wireless sensor networks," in *2016 IEEE SENSORS*, Oct 2016, pp. 1–3.
[19] Orange, "LoRa device developer guide," April 2016.
[20] GSMA, "3GPP low power wide area technologies, GSMA white paper," Tech. Rep., October 2016.

[21] C. Gezer, C. Buratti, and R. Verdone, "Capture effect in IEEE 802.15.4 networks: Modelling and experimentation," pp. 204–209, May 2010.
[22] A. F. Molisch, *Wireless communications*. John Wiley & Sons, 2007.
[23] M. Gudmundson, "Correlation model for shadow fading in mobile radio systems," *Electronics Letters*, vol. 27, no. 23, pp. 2145–2146, Nov 1991.